HARMONIC DISTURBANCES UP TO 150 KHZ PRODUCED BY SMALL WIND TURBINES ON THE LV DISTRIBUTION GRID

Caroline LEROI
Université catholique de Louvain
Belgium
caroline.leroi@uclouvain.be

Emmanuel DE JAEGER
Université catholique de Louvain
Belgium
emmanuel.dejaeger@uclouvain.be

Marc BEKEMANS
Thales Alenia Space
Belgium
marc.bekemans@thalesaleniaspace.com

ABSTRACT

This paper presents harmonic computations for four different configurations of wind turbines. The first part of the paper will be dedicated to a presentation and discussion of the models developed to study by simulation the disturbances produced by small wind turbines. The second part of the paper describes which harmonics are found on the grid side of the wind turbine. The third part of the paper concerns the presentation of several simulation results. These simulations study the impact of the active power on the level of disturbances.

INTRODUCTION

In the context of global warming, particular attention is drawn on renewable energies and their impact on the grid. One of the most promising renewable energy sources are the wind turbines. The power produced by wind turbines can vary from a few kW to several MW. The impact on the grid will be different as the smaller ones are connected to the Low Voltage (LV) distribution grid while the bigger ones are connected to the Medium Voltage grid through a transformer. This paper will be focused on small wind turbines (i.e. less than 100 kW) and their impact on the LV distribution grid, as far as harmonic disturbances are concerned.

Small wind turbines are usually made of a Permanent Magnet Synchronous Generator (PMSG) with a full power converters chain. This power converters chain induces mostly two kinds of disturbances. First of all, there are interharmonics in the low frequencies which are linked to the rotor speed. The other disturbances are harmonics due to the inverter switching frequency. This switching frequency is usually equal to a few kHz.

It has already been shown in [1] that interharmonics due to the rotor speed are correlated with the active power produced by the wind turbine. In [1] conclusions are based on measurements from three individual wind turbines (2 and 2.5 MW size).

In this paper the research made in [1] is extended to small wind turbines and on high frequencies harmonics (up to 150 kHz). Indeed, harmonics produced by the inverter switching frequency will be found in the frequency range 2-150 kHz. Electromagnetic interference due to conducted disturbances in this frequency range has become a real issue in the context of public LV distribution grids. Therefore, it is useful to extend the research to that frequency range.

Results will be based on modelling and simulations performed with Matlab Simulink environment and more specifically the SimPowerSystems toolbox. The simulated generator is a PMSG with a rated power of 50 kW. Two different power converters chains will be simulated. Firstly, a diode rectifier followed by a boost and an inverter. This is the most common topology for small wind turbines as it is simple and cheap. The other simulated topology is back-to-back PWM converters, i.e. an active rectifier followed by an inverter.

The paper will also study the impact of the chosen filter configuration. It will be limited to the two most common filters: L-filter and LCL filter with a damping resistor in series with the capacitor.

MODELS

Models have been developed in order to study the impact of small wind turbines on harmonics injected into the grid. These models can be divided in 5 parts that will be described separately: the turbine, the generator, the power converters chain, the filter and the grid.

Turbine

The wind turbine input is the mechanical torque which is given by equation (1).

$$T_m = \frac{1}{2}\rho A C_p v_{wind}^3 \frac{1}{\omega_r} \quad (1)$$

ρ is the air mass density, A is the section of area swept out by the wind turbine blades, C_p is the power coefficient, v_{wind} is the wind speed and ω_r is the rotor angular speed. Parameters of the wind turbine Fairwind F180-50 are chosen [2]. This wind turbine has a rated power of 50 kW at a wind speed of 11m/s. An approximated curve which fits to the characteristics of the F180-50 has been developed.

Generator

The generator is modelled by the block Permanent Magnet Synchronous Generator available in the SimPowerSystems library. This blocks requires several parameters that are not publicly available (e.g. stator resistance, armature inductance, flux linkage established by magnets). Those parameters cannot be fixed arbitrarily as they have a big influence on the wind turbine performance. This can be observed in Figure 1 which illustrates the mechanical and electrical power in function of the rotor speed for different electrical parameters and

for a wind speed of 11m/s. The electrical power curves shown in this figure have been computed.

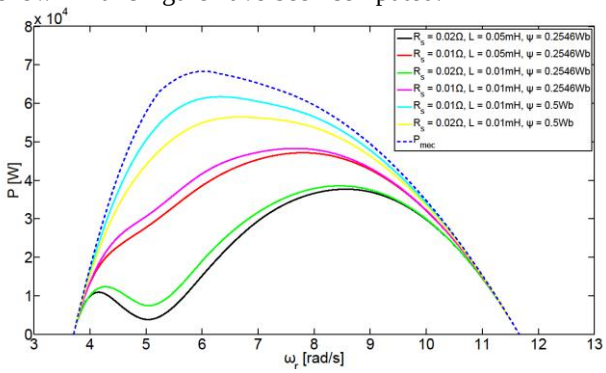

Figure 1 Mechanical and electrical power in function of the rotor speed for different electrical parameters

Since the simulated wind turbine is supposed to have a rated power of 50 kW, parameters leading to the yellow curve have been chosen. It can also be noticed in Figure 1 that mechanical and electrical power are not optimal for the same rotor speed. This is a characteristic of small wind turbines that has already been discussed in [3].

Power converters chain

Two different power converters chains have been simulated. Firstly, a diode rectifier followed by a boost and an inverter. This is the most common topology for small wind turbines as it is simple and cheap. The other simulated topology is back-to-back PWM converters, i.e. an active rectifier followed by an inverter. Both solutions have a converter on the generator side whose control aims to extract maximum power and a converter on the grid side which controls the DC voltage and the reactive power injected into the grid. To track the maximum power, the power mapping method has been implemented [4].

Filter

Two filters topologies have been studied and compared: L-filter and LCL filter with a damping resistor in series with the capacitor. The inductance of the L-filter has been fixed to 10 mH because it was the best compromise between a low voltage drop and a good attenuation of high frequency harmonics. Concerning the damped LCL-filter, it has been designed using the method described in [5]. It gives an inductance of 4.3mH on the converter side, of 0.34mH on the grid side, a capacitance of 50µF and a damping resistance of 0.8342Ω.

Figure 2 shows the transfer function between the voltage at the input of the filter and the current at its output. The inverter in both converters configurations has a switching frequency of 3 kHz. Therefore, harmonics at the switching frequency and at its multiples are more attenuated by the LCL filter than by the L filter.

LV grid

The grid is represented by a voltage source and a short

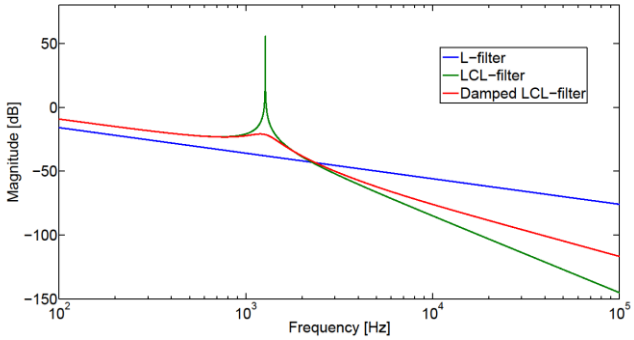

Figure 2 Bode diagram of the transfer function $\frac{\bar{I}_{out}}{\bar{V}_{in}}$

circuit impedance. This model is not really suitable for HF studies and should be improved to study the propagation of HF disturbances. The line voltage fixed by the voltage source is 400V since it is low voltage grid. The resistance is 0.032Ω and the reactance is 0.00688Ω. This impedance corresponds to a short-circuit power of about 5MVA and a ratio $\frac{X}{R}$ of about $\frac{1}{5}$. They are parameters of a typical industrial grid with 100m of XVB cable.

Figure 3 and Figure 4 illustrate the two different power converters chains that have been simulated.

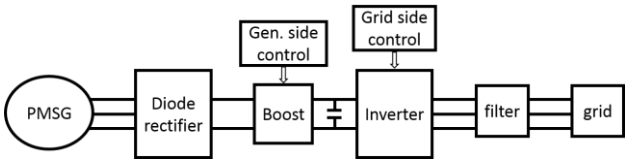

Figure 3 A diode rectifier with an intermediate DC/DC converter stage and an inverter

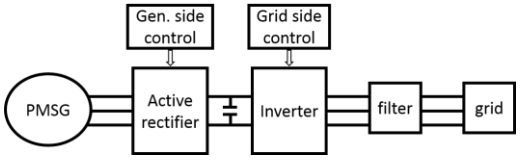

Figure 4 Back-to-back converters

HARMONICS

Due to the power converters chain, harmonics will be found on the grid side.

For the configuration with the boost, there are three different sources of harmonics. First of all, there are interharmonics linked to the rotor speed. If f_1 is the frequency on the stator side and f_0 is the grid frequency, interharmonics are found at frequencies equal to $6f_1 \pm f_0$, $6f_1 \pm 5f_0$, $6f_1 \pm 7f_0$, $12f_1 \pm f_0$, etc. [6].

Figure 5 shows the spectrum of the current up to 300Hz when the active power is about 20% of the nominal power. The stator frequency is equal to 12.58Hz. Therefore, the peaks observed around 25Hz and around 125Hz correspond to $6f_1 \pm f_0$, the ones around 100Hz and 200Hz to $12f_1 \pm f_0$, etc. Harmonic 5 is also observed but its value is lower than the higher interharmonics.

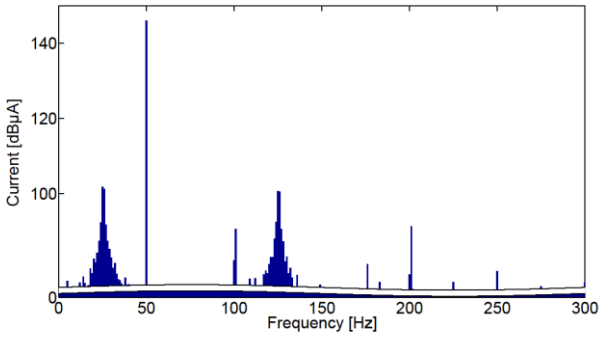

Figure 5 Spectrum of the current when the active power is about 0.2 per unit for the configuration with the boost and the L filter.

The second source of harmonic is due to the switching frequency of the boost. Since it has been fixed to 10kHz, harmonics around 10kHz are found on the grid side.
The last source is the inverter. Its switching frequency has been fixed to 3kHz. Therefore, harmonics around 3kHz, 6kHz, 9kHz, etc. will be observed on the grid side. In particular, if f_s is the switching frequency and f_0 is the grid frequency, harmonics are found at frequencies equal to $f_s \pm 2f_0$, $f_s \pm 4f_0$, $2f_s \pm f_0$, $2f_s \pm 3f_0$, $3f_s \pm 2f_0$, $f_s \pm 2f_0$, etc. Harmonics multiple of 3 are not present since $\frac{f_s}{f_0}$ is a multiple of 3. The inverter induces also harmonics $5f_0$, $7f_0$, $11f_0$, $13f_0$, etc.
Figure 6 shows the spectrum of the current up to 20kHz when the active power is about 20% of the nominal power. Harmonics around the multiple of the switching frequency of the inverter are clearly visible. Harmonics around the switching frequency of the boost, i.e. 10kHz are very small.

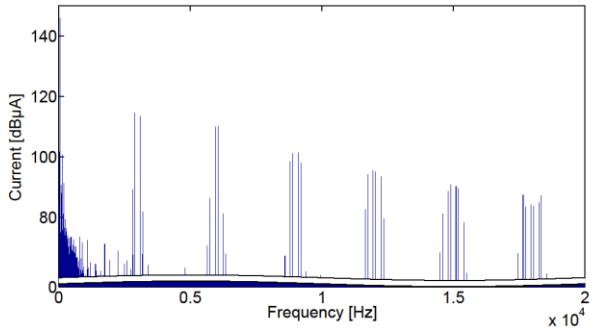

Figure 6 Spectrum of the current when the active power is about 0.2 per unit for the configuration with the boost and the L filter.

For the back-to-back configuration, there are two different sources of harmonics. The first one is the active rectifier. It is controlled by Pulse Width Modulation (PWM) which is synchronized with the stator frequency. The ratio between the carrier frequency and the stator frequency has been fixed to 600 leading to a switching frequency varying from 5kHz to 13.5kHz. Harmonics around this switching frequency are found on the grid side. The active rectifier induces also the same interharmonics as the diode rectifier. The second source is the inverter and it generates the same disturbances as in the configuration with the boost.

SIMULATION RESULTS

As it has been seen in the previous section, wind turbines produce mostly two kinds of disturbances. Harmonics in the high frequency range due to the inverter and interharmonics in the low frequency range linked to the rotor speed. Harmonics due to the boost are negligible compared to harmonics of the inverter. It is also true for HF harmonics produced by the active rectifier in the back-to-back configuration. This is probably due to the high capacitance on the DC link. In the low frequency range, interharmonics linked to the rotor speed are also higher than LF harmonics due to the inverter. Therefore, the simulation results presented in this section will only concern harmonics around the multiple of the switching frequency of the inverter and interharmonics $6f_s \pm f_0$.
Simulations have been performed for wind speed ranging from 4m/s to 11m/s with a step of 1m/s. Values at 10.25m/s and 10.5m/s have also been registered. For each wind speed, the power_fftscope function of Matlab has been used to compute the different harmonics. The presented results come from different steady-state simulations at different wind speeds. A window of 1s has been chosen in order to have a value each Hertz. This accuracy is necessary to compute the interharmonics.
Both current and voltage harmonics will be analysed. They will be expressed in dBµA and dBµV respectively.

HF disturbances produced by the inverter

It has been seen in Figure 6 that the inverter induces harmonics around multiples of its switching frequency. The study will be limited to the three first groups of harmonics, that is to say, harmonics around the switching frequency of the inverter, around twice this switching frequency and around three times this frequency. For each subgroup of harmonics, a quadratic sum ($\sqrt{\sum_i x_i^2}$) will be performed on the 6 harmonics closest to the central frequency (e.g. for the subgroup around the switching frequency, the quadratic sum is performed on harmonics at 2900Hz, 3100Hz, 2800Hz, 3200Hz, 2600Hz and 3400Hz). Results will show the evolution of the quadratic sum of each subgroup with the active power for the four configurations: two different filters, L and LCL and two different power converters chains, configuration with the boost and the back-to-back. Computations are performed after the filter.

Current harmonics

Figure 7, Figure 8 and Figure 9 show the evolution with the active power of the quadratic sum of current harmonics around the switching frequency, twice the switching frequency and three times the switching frequency.
Several observations can be done from these figures.

- Both configurations give almost the same results. In

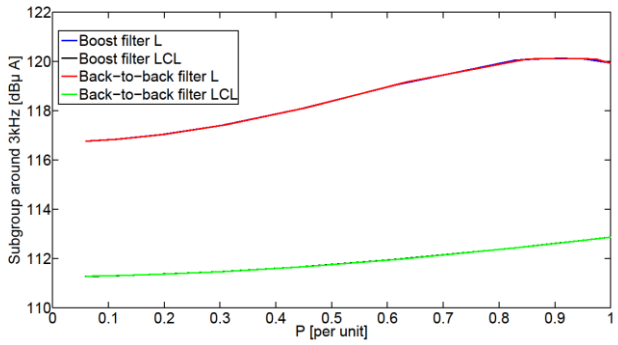

Figure 7 Quadratic sum of the current harmonics around the switching frequency in function of the active power

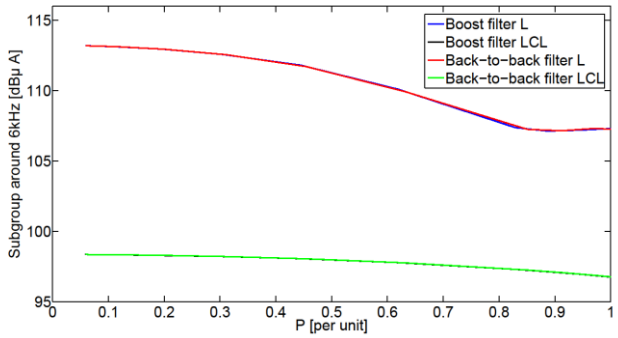

Figure 8 Quadratic sum of the current harmonics around twice the switching frequency in function of the active power

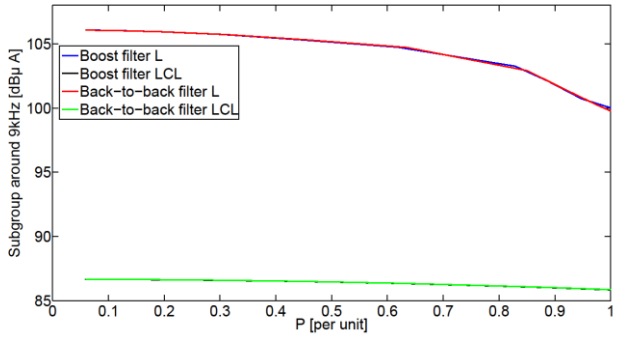

Figure 9 Quadratic sum of the current harmonics around three times the switching frequency in function of the active power

fact, they have the same inverter, therefore, the rectifier configuration has no impact on the high frequency disturbances produced by the inverter.

- It is confirmed that the LCL filter attenuates more the high frequency disturbances than the L filter. It could already have been concluded from Figure 2. Furthermore, the difference between the two filters increases with the frequency.
- The current harmonics around the switching frequency seem to increase with the active power while they decrease for the higher frequencies.

The maximum disturbance is about 120.1dBµA around 90% of the nominal power.

Voltage harmonics

Figure 10, Figure 11 and Figure 12 show the evolution with the active power of the quadratic sum of voltage harmonics around the switching frequency, twice the switching frequency and three times the switching frequency.

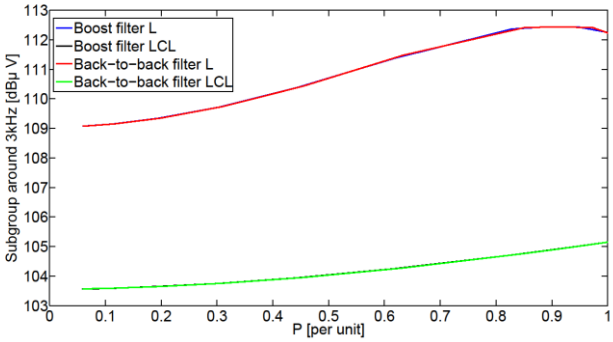

Figure 10 Quadratic sum of the voltage harmonics around the switching frequency in function of the active power

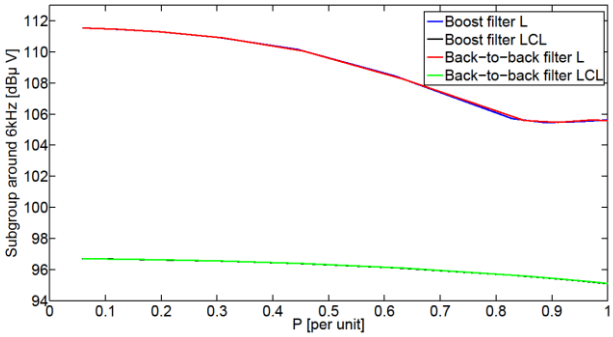

Figure 11 Quadratic sum of the voltage harmonics around twice the switching frequency in function of the active power

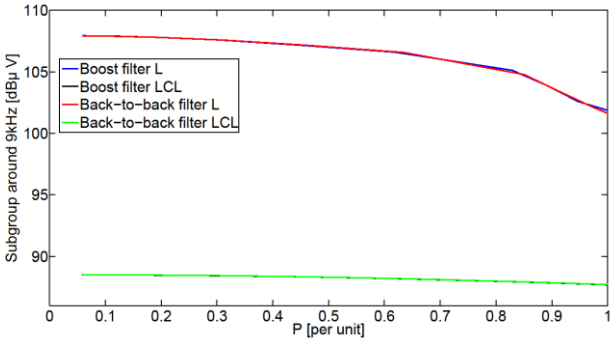

Figure 12 Quadratic sum of the voltage harmonics around three times the switching frequency in function of the active power

Observations are the same than for the current harmonics. The curves shapes are identical because a simple grid model has been used. The maximum disturbance is about 112.4dBµV at around 90% of the active power.

LF disturbances linked to the rotor speed

In this section, results concerning the disturbances linked to the rotor speed will be presented. It has been seen in Figure 5 that, in the low frequency range, highest interharmonics are around $6f_1 \pm f_0$. A quadratic sum will be performed on the subgroup around $6f_1 + f_0$. The interharmonic $6f_1 + f_0$ and the 4 interharmonics closest to it will be taken into account in the summation. Results will show the evolution with the active power of this quadratic sum for the four configurations.

Current harmonics

Figure 13 shows the evolution with the active power of the quadratic sum of current interharmonics around $6f_1 + f_0$.

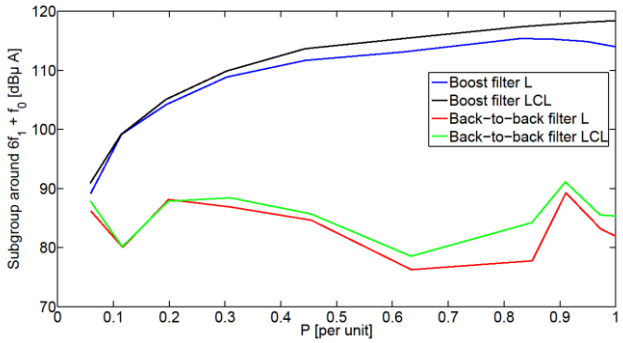

Figure 13 Quadratic sum of the current interharmonics around $6f_1 + f_0$ in function of the active power

Results for the configuration with the boost shows that the LF disturbances clearly increase with the active power. It is less obvious for the back-to-back configuration. It could be because the synchronization of the PWM with the stator frequency is not perfectly performed. It should also be noted that interharmonics might be underestimated since the accuracy of the FFT is 1Hz.

It can also be noticed from Figure 13 that the LF disturbances are higher when the LCL filter is used. This can be explained by the Bode diagram of Figure 2.

The higher disturbance occurs at nominal power and is equal to 118.7dBµA.

Voltage harmonics

Figure 14 shows the evolution with the active power of the quadratic sum of voltage interharmonics around $6f_1 + f_0$.

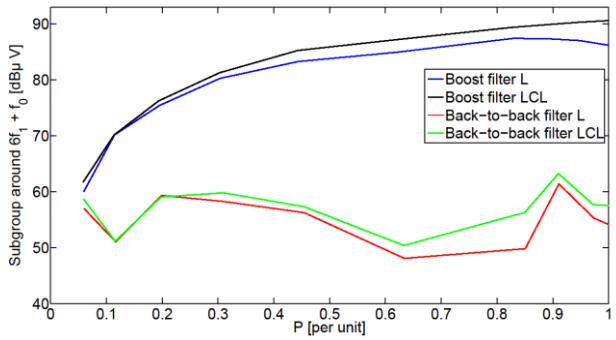

Figure 14 Quadratic sum of the voltage interharmonics around $6f_1 + f_0$ in function of the active power

Conclusions are the same than for the current. The maximum disturbance occurs also at nominal power and is equal to 91.03dBµV.

CONCLUSION

The issue concerning HF and LF disturbances produced by small wind turbines has been dealt with. Four different models have been established in order to study these disturbances by simulation. A good knowledge of the generator's electrical parameters is key, due to the high sensitivity of the electrical power characteristic with respect to these parameters. Furthermore, for small wind turbines, the mechanical optimum does not necessarily correspond to the electrical optimum.

From the simulation results, it can be concluded that the LCL filter attenuates more HF disturbances than the L filter but the LF disturbances are higher with this filter.

Concerning the HF disturbances, the circuit upstream from the inverter has no impact since the results are the same for the configuration with the boost and for the back-to-back. Moreover, HF disturbances produced upstream from the inverter are almost no more present on the grid side.

Finally, the level of disturbances seems to increase with the active power for the harmonics around the switching frequency of the inverter and for the interharmonics linked to the rotor speed while it decreases for higher order harmonics. All results presented in this paper are based on models which should be checked through experiments on a real grid.

Acknowledgments

This work was partially financed in the framework of an industrial research project with the *ENGIE* group.

REFERENCES

[1] K. Yang, M.H.J. Bollen, E.A. Larsson and M. Wahlberg, 2014, "Measurements of Harmonic Emission versus Active Power from Wind Turbines", *Electric Power Systems Research*, vol.108, 304-314.

[2] Fairwind, "F180-50 Main technical data", http://www.fw4sea.com/en/

[3] C. Vlad, I. Munteanu, A.I. Bratcu and E. Ceanga, 2010, "Output power maximization of low-power wind energy conversion systems revisited: Possible control solutions", *Energy conversion and management*, vol. 51, 305-310.

[4] K. Tan, S. Islam, 2004, "Optimum control strategies in energy conversion of PMSG wind turbine system without mechanical sensors", *IEEE transactions on energy conversion*, vol.19, 392-399.

[5] A. Reznik, M. G. Simoes, A. Al-Durra and S. M. Muyeen, 2012, "LCL filter design and performance analysis for small wind turbine systems", *Proceedings Power Electronics and Machines in Wind Applications (PEMWA)*, IEEE, 1-7.

[6] K. Yang, 2015, "On harmonics emission, propagation and aggregation in wind power plants", Doctoral thesis, Lulea university of technology.